Article

Electrochemistry of the Self-Assembled Monolayers of Dyads Consisting of Tripod-Shaped Trithiol and Bithiophene on Gold

Toshikazu Kitagawa [1,*], Hiroaki Matsubara [2], Takao Okazaki [1] and Koichi Komatsu [2]

[1] Department of Chemistry for Materials, Graduate School of Engineering, Mie University, Tsu, Mie 514-8507, Japan

[2] Institute for Chemical Research, Kyoto University, Uji, Kyoto 611-0011, Japan

* Author to whom correspondence should be addressed; E-Mail: kitagawa@chem.mie-u.ac.jp; Tel./Fax: +81-59-231-9416.

Abstract: Self-assembled monolayers (SAMs) of tripod-shaped trithiols, consisting of an adamantane core with three CH_2SH legs and a bithiophene group, were prepared on a Au(111) surface. Adsorption in a tripod-like fashion was supported by polarization modulation-infrared reflection absorption spectroscopy (PM-IRRAS) of the SAMs, which indicated the absence of free SH groups. Cyclic voltammetry showed an irreversible cathodic wave due to reductive desorption. The SAM also showed an anodic wave due to the single-electron oxidation of the bithiophene moiety without concomitant desorption of the molecules. Although oxidation was irreversible in the absence of a protecting group, it became reversible with the introduction of a terminal phenyl group. The charge of the oxidation was one-third that of the reductive desorption, confirming a three-point adsorption. The surface coverage was *ca*. 50% of that expected for the *anti* bithiophene conformation, which suggested that an increase in the surface area per molecule had been caused by the presence of an energetically high-lying *syn* conformer. In accordance with this, the line shape of the oxidation wave suggested an electrostatic repulsive interaction between neighboring molecules.

Keywords: self-assembled monolayer; molecular tripod; bithiophene; adamantane; cyclic voltammetry

1. Introduction

The tight binding of a sulfur atom in an organic molecule to a metal gold surface provides a secure and facile way to prepare a self-assembled monolayer (SAM) [1–4], which allows a reliable means for interface functionalization. A variety of monolayers, prepared from properly designed thiols and bisulfides, have been extensively studied for applications to sensors [5–7], molecular machines [8–11] and molecular electronic devices [12–22].

Tripod-shaped molecules that have three legs with a terminal sulfur group at the end of each leg can serve as tight-binding anchors for the construction of SAMs [8,17–34]. Previously, we reported that molecular tripod **1**, composed of a rigid adamantane core and three CH_2SH legs [23,24,27], forms a SAM on Au(111) with a highly ordered arrangement by three-point adsorption (Figure 1). We further succeeded in preparing a trithiol with terminal ferrocene **2**, in which the ferrocenyl group was connected with an adamantane tripod through a linear phenyleneethynylene linker [25–27]. Due to the area-demanding tripod structure, **2** enabled the formation of a SAM with "ideal" behavior, where no electrostatic interaction among surface ferrocenyl groups was present, which is otherwise difficult to realize without the help of non-electroactive diluting molecules.

Figure 1. Structures of tripod-shaped trithiols with an adamantane core. The structures of **3a** and **3b** represent *anti* conformers.
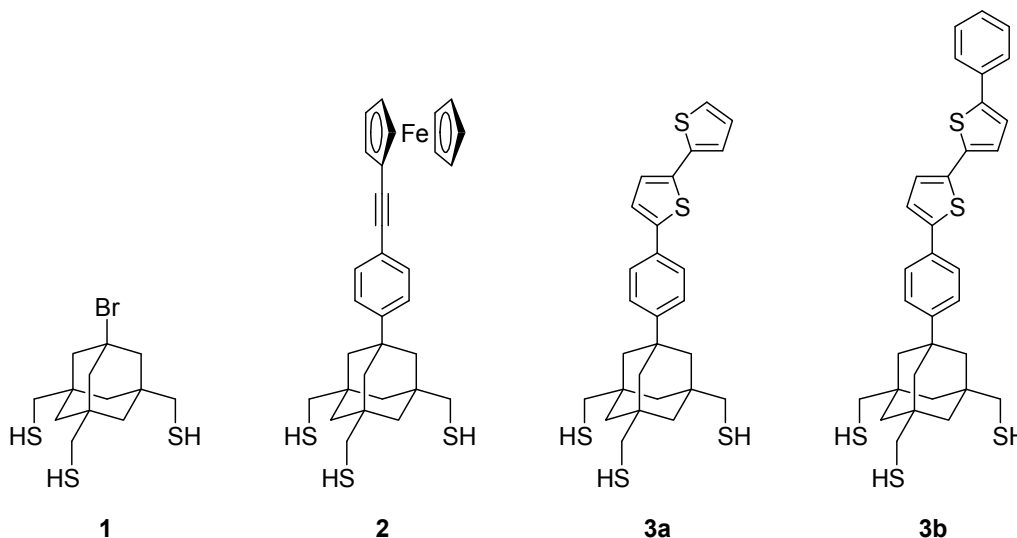

In the present study, we synthesized dyads **3a** and **3b**, which consist of another electroactive molecule, bithiophene, connected with the adamantane tripod, and investigated the electrochemistry of their SAMs. SAMs of oligothiophenes with a monodentate anchor [20,35,36], bidentate anchor [37] or triarylmethyl tripod anchor [17–22] have been used in the construction of molecular electronic devices, such as photovoltaic cells and light-emitting diodes. Oligothiophenes with an all-*anti* (all-transoid) conformation can adopt a near-perpendicular orientation in SAMs, while the presence of a *syn*-linkage could prevent dense packing because of its bent structure. Since **3a** and **3b** have no alkyl side chains on the thiophene rings, their *anti* conformers form SAMs with potentially the same surface density as that of **1** and **2**. Thus, reduced surface coverages of tripods **3**, if observed, could be good indicators for the presence of *syn*-linked bithiophene in SAMs (Figure 2).

Figure 2. Schematic representation of a SAM of *anti*-**3b** containing the *syn*-conformer.
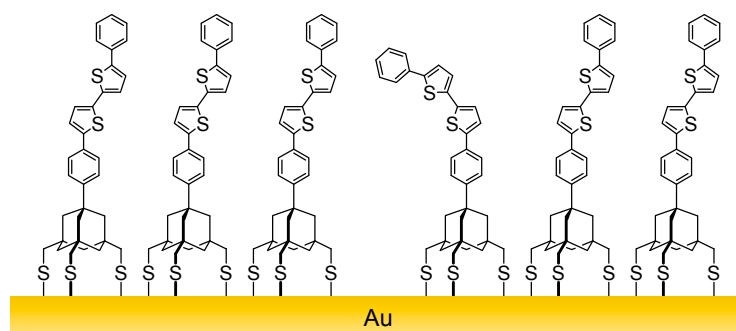
2. Results and Discussion

2.1. Synthesis of Tripodal Trithiol–Bithiophene Dyads

Tripod-linked bithiophenes **3a** and **3b** were prepared via the Stille coupling of *p*-iodophenyl tris(thioacetate) **4** [23,26] with the corresponding 2-tributylstannylated bithiophenes, **5a** and **5b**, followed by deprotection of the thiol groups (Scheme 1). Unlike the good-to-fair yields that have been reported for the Stille coupling of stannylbithiophene [38–40], the reactions with **5** were relatively poor, which could be ascribed to possible catalyst poisoning by the sulfur atoms in the legs. Reduction of the acetylthio groups of **6** by LiAlH₄ afforded the target trithiols **3a** and **3b** in good yields. The reactions were so clean, that the products could be obtained in a pure form with no purification (**3a**) or after simple flash chromatography (**3b**). Further purification by HPLC was not beneficial, owing to a significant loss of the sample, due to the immobilization of the molecules on the inner surface of the stainless-steel column during separation.

Scheme 1. Synthesis of trithiols **3a** and **3b**.
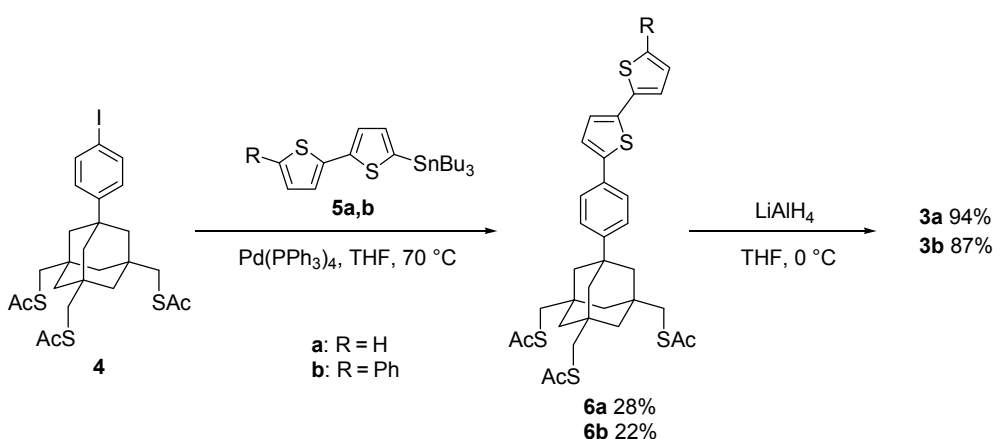
2.2. Formation of the SAM of **3** and Characterization by PM-IRRAS

The SAMs of tripods **3a** and **3b** were prepared by immersing a Au(111) substrate, prepared by depositing gold on a mica sheet, into 0.1 mM solutions in ethyl acetate (**3a**) or dichloromethane (**3b**) at ambient temperature for 24 h or longer. The SAM-modified substrate was washed thoroughly with the same solvent and air-dried.

The infrared reflection absorption spectrum (IRRAS) of the SAMs, recorded in a polarization modulation mode (PM), showed no distinct peak of the S–H stretching vibration, which was seen at *ca*. 2570 cm^{-1} in the infrared spectrum of the neat samples of **3** (Figure 3). This is consistent with the formation of SAMs using all three sulfur legs, which leads to a perpendicular orientation of the molecules. The peaks of antisymmetric and symmetric CH$_2$ stretching, which were observed at around 2915 and 2848 cm^{-1}, respectively, for neat samples, were shifted to higher wavenumbers by 7–11 cm^{-1} in the SAMs. These shifts might indicate the tightening of the C–H bonds due to the fixation of the three legs on the Au surface.

Figure 3. Infrared absorption spectra of trithiols **3a** (**A**) and **3b** (**B**): upper spectra, transmission spectra for drop-cast films prepared on a KBr plate using CHCl$_3$ solutions; lower spectra, polarization modulation-infrared reflection absorption spectroscopy (PM-IRRAS) spectra for the thiolate SAMs on Au(111).
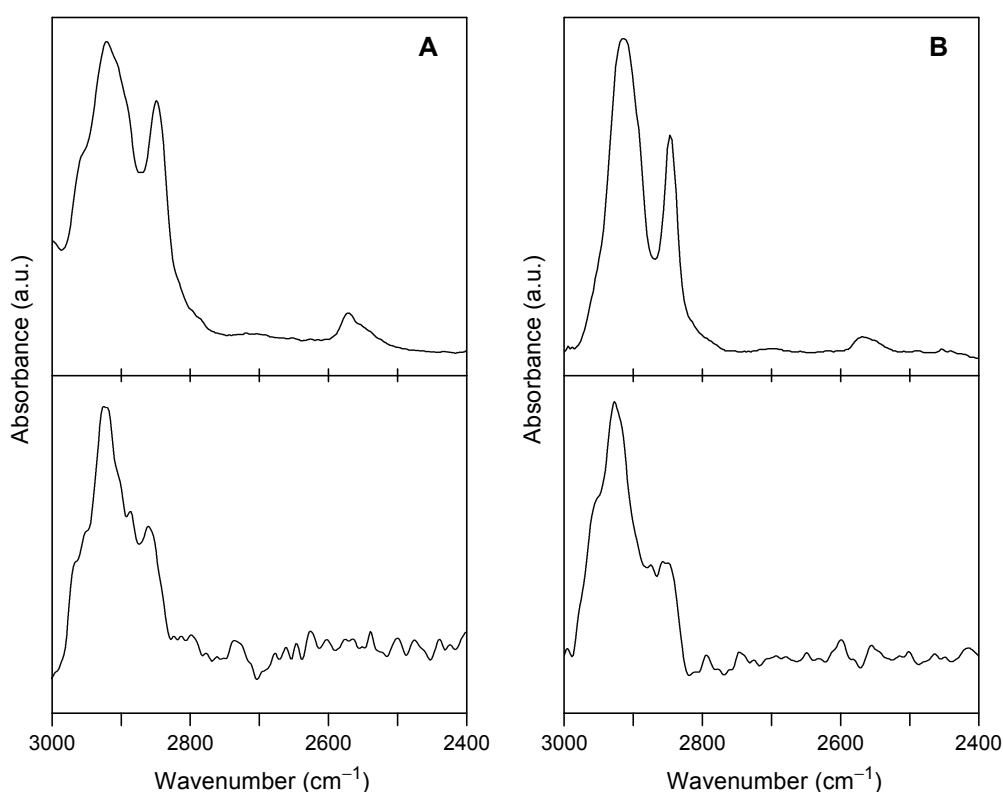
2.3. Electrochemistry of the SAM of **3**

2.3.1. Reductive Desorption

The cyclic voltammetry of the SAMs of **3a** and **3b** in aqueous KOH (Figure 4) showed irreversible reduction peaks at −1.057 and −1.085 V (*vs.* Ag/AgCl), respectively, due to the reductive desorption of the thiolate ion [41–47]:

$$RS–Au(s) + e^{-} \rightarrow RS^{-} + Au(s) \tag{1}$$

A small oxidation wave at approximately −0.84 V was also observed due to a readsorption of the thiolate ion [43–45].

The peak potential (E_p), the charge of the reductive wave (Q_{red}) and the full width at half-maximum (ΔE_{fwhm}) are listed in Table 1, together with the values for related SAMs. The SAMs of long-chain *n*-alkanethiols are known to show a large negative E_p (<-1.0 V), because the adsorbed molecules resist desorption due to strong attractive interactions between van der Waals-contacting alkyl groups [46]. On the other hand, the large negative E_ps for the SAMs of tripod molecules **1**–**3** should be rather attributed to the tight binding of the molecules to the substrate by the three S–Au bonds.

Figure 4. Reductive desorption of the SAMs of **3a** (**A**) and **3b** (**B**) on Au(111), as observed by cyclic voltammetry using the surface-modified gold substrate as a working electrode in 0.5 M aqueous KOH: geometric area of the working electrode, 0.152 cm^2; scan rate, 0.02 V·s^{-1} for **3a** and 0.1 V·s^{-1} for **3b**.
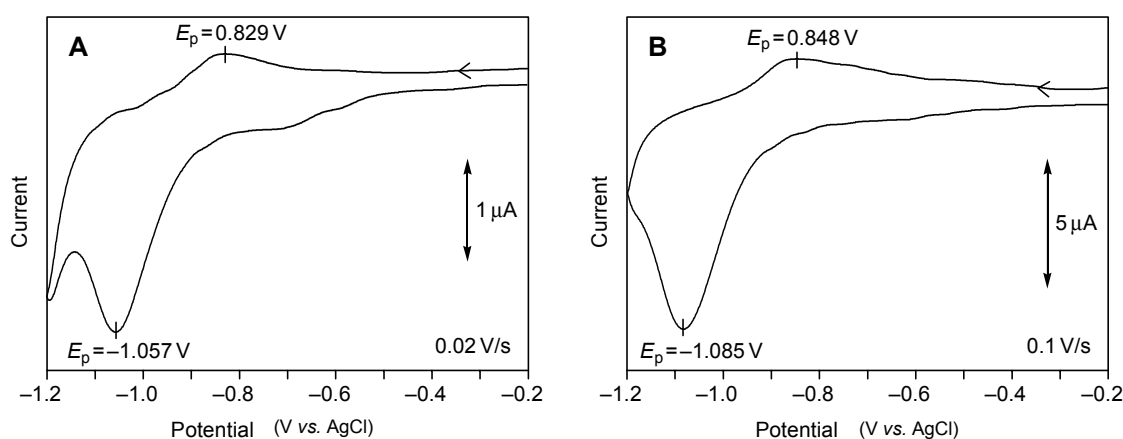

Table 1. Peak potential (E_p), charge (Q_{red}) and full width at half-maximum (ΔE_{fwhm}) for the reductive desorption of thiol SAMs on Au(111), as measured by cyclic voltammetry [a].

Thiol	E_p (V *vs.* Ag/AgCl)	Q_{red} [b] (µC·cm^{-2})	ΔE_{fwhm} (mV)
1 [c]	−1.088	100	91
2 [d]	−0.977	91	125
3a	−1.057	51	108
3b	−1.085	49	121
n-C$_{12}$H$_{25}$SH [c]	−1.084	100	20

[a] In 0.5 M aqueous KOH; [b] calculated from the reduction peak area. The uncertainty due to sample-to-sample variations is ±10%; [c] [23]; [d] [26].

The small ΔE_{fwhm} for *n*-dodecanethiol can also be ascribed to the strong attractive interaction between neighboring alkyl chains [46], while the much larger values observed for tripod trithiols indicate the insignificance of such interactions.

The surface coverage of the adsorbed molecules (Γ_{red}) is proportional to Q_{red}:

$$\Gamma_{red} = Q_{red}/nFA \qquad (2)$$

Here, $n = 3$ electrons per molecule, F is the Faraday constant and A is the geometric area of the electrode (0.152 cm^2). As indicated in Table 1, we previously reported [23,26] that the SAMs of bromine- and ferrocene-terminated trithiols (**1** and **2**) showed Q_{red}s of *ca.* 100 µC·cm^{-2}, which

approximated that observed for *n*-dodecanethiol. On the other hand, the reductive charges of **3a** and **3b** were approximately 50 $\mu C \cdot cm^{-2}$, which may be explained by the greater area per molecule due to the bulky bithiophene moiety.

Figure 5 shows the density functional theory (DFT)-optimized structures of **3b** with *anti* and *syn* conformations. The former had a near-perpendicular structure, while the latter was bent to a large extent and was 1.5 $kJ \cdot mol^{-1}$ higher in Gibbs energy than the former [48]. The dihedral angles between the mean planes of adjacent benzene and thiophene rings were constant within a range of 23°–27° in both structures, while those between two directly bound thiophene rings showed a large difference (*anti*: 18.5°, *syn*: 26.3°), due to the steric repulsion between the hydrogen atoms in *syn*-bithiophene. The *anti* conformation would be more favorable in SAMs, because of not only its lower energy, but also its small occupied area, which allows for higher surface coverage. However, the small *anti-syn* energy difference may allow some fraction of molecules to adopt the *syn* conformation.

Figure 5. DFT-optimized structures of *anti* and *syn* conformers of trithiol **3b** calculated at the B3LYP/3-21G(d) level. The dihedral angles between adjacent rings are shown. Lower structures represent top views, with the diphenylbithiophene moiety highlighted in light blue.
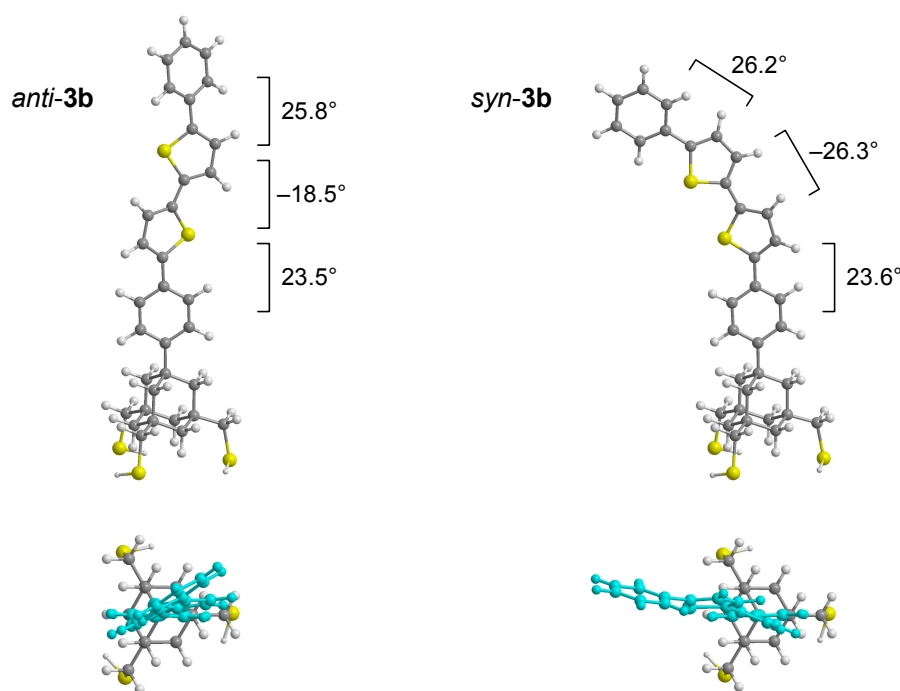

Since adsorbate **3a** is less bulky than **3b**, the observed similar coverages of their SAMs would be due to either a greater *syn/anti* ratio or less complete adsorption of **3a**. However, the latter possibility can be ruled out, because the surface coverage was not changed by prolongation of the SAM preparation time.

2.3.2. Oxidation of the Bithiophene Moiety

Cyclic voltammetry was performed in a positive potential range in CH_2Cl_2 to examine the oxidation process of the bithiophene moiety. The SAM of **3a** showed an irreversible oxidation wave at 1.017 V (*vs.* Ag/AgNO₃), corresponding to single-electron oxidation of the bithiophene moiety (Figure 6A).

This wave disappeared in the second cycle, but a subsequent voltammetry over −0.2 to −1.2 V in aqueous KOH using the same substrate showed a reductive wave (Q_{red} = 48 $\mu C \cdot cm^{-2}$) similar to that in Figure 4B (data not shown). These results rule out desorption during electrochemical oxidation and suggest that the bithiophene group underwent decomposition after single electron oxidation. Since oxidative coupling is prohibited for a surface-confined monolayer, it is more likely that the radical cation was captured by molecular oxygen, followed by ring cleavage [49]. The peak area of the oxidative wave corresponded to a charge of 16 ± 2 $\mu C \cdot cm^{-2}$.

Figure 6. Cyclic voltammograms of the SAMs of **3a** (**A**) and **3b** (**B**) recorded in CH2Cl2: geometric area of the working electrode, 0.152 cm^2; scan rate, 0.1 $V \cdot s^{-1}$ for **3a** and 0.2 $V \cdot s^{-1}$ for **3b**. Tetrabutylammonium perchlorate (TBAP) (0.1 M) was used as a supporting electrolyte.
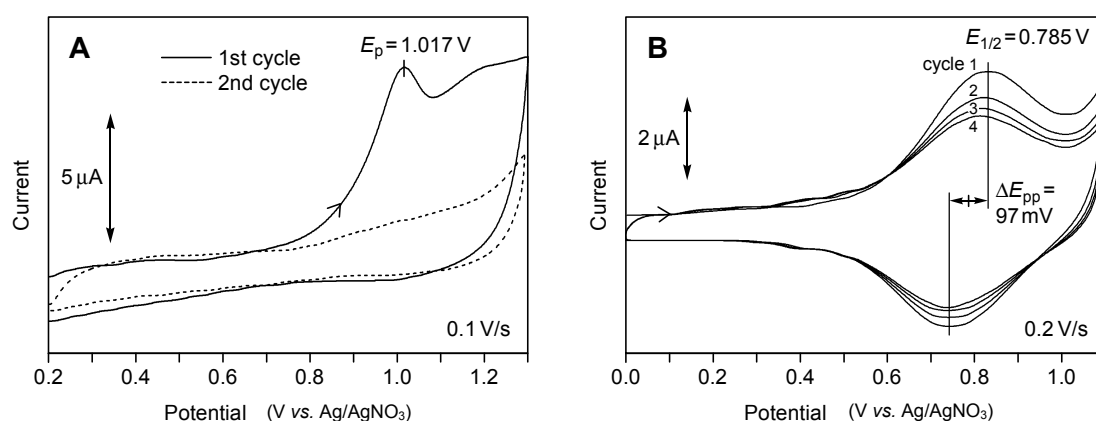

An oxidative scan of the SAM of **3b**, however, showed a reversible wave at $E_{1/2}$ = 0.785 V (*vs.* Ag/AgNO3) with a charge of 17 ± 2 $\mu C \cdot cm^{-2}$ (Figure 6B). The anodic to cathodic peak separation (E_{pp} = 97 mV) and the full width at half-maximum (E_{fwhm} = 260 ± 20 mV) were considerably greater than those expected for an "ideal" Nernstian redox system: E_{pp} = 0 and E_{fwhm} = 3.53RT/nF (90.6 mV at 25 °C and n = 1) [50]. This was in contrast to the result for the SAM of **2**, which demonstrated ideal behavior as a result of the absence of the electrostatic interaction between neighboring ferrocenyl groups [26]. Large E_{pp}s and E_{fwhm}s have been commonly observed for other densely packed electroactive SAMs due to lateral molecular interaction [51–53]. In the present SAMs, such an interaction would be enhanced by the presence of the area-demanding *syn* conformer.

In Figure 6B, a *ca.* 7% decrease in the peak current was observed with each cycle. This is probably due to the partial desorption of the molecule, since a reductive desorption measurement after the fourth cycle showed a charge that was 40% less than that observed in Figure 4A [54].

For both **3a** and **3b**, the oxidative charge (16–17 $\mu C \cdot cm^{-2}$) was one-third of that observed for reductive desorption (Table 1), which was consistent with the 3:1 ratio of the densities of a S–Au bond and the bithiophene group, thus further confirming the achievement of three-point adsorption. The observed reversible behavior indicated that the phenyl end cap effectively improved the stability of the radical cation. In this context, the oxidized species from the parent bithiophene was reported to be stabilized by the capping with two terminal phenyl groups in solution [55]. The cyclic voltammetry of tris(thioacetate) **6b** in solution (Figure 7) also showed a reversible first oxidation wave ($E_{1/2}$ = 0.740 V)

and an irreversible second one (E_{pa} = 1.180 V). In the case of the SAM of **3b**, however, only the first oxidation wave was observed, because the oxidative desorption of a sulfur atom, RS–Au(s) + 2H$_2$O → Au(s) + RSO$_2$H + 3e$^-$ + 3H$^+$ [42], occurred at potentials higher than 1.1 V.

Figure 7. Cyclic voltammograms of a CH$_3$CN solution of **6b** (1 mM) recorded over two different potential ranges. Ferrocene (1 mM) was added as a current standard: scan rate, 0.1 V·s^{-1}; working electrode, glassy carbon; counter electrode, Pt wire. TBAP (0.1 M) was used as a supporting electrolyte.
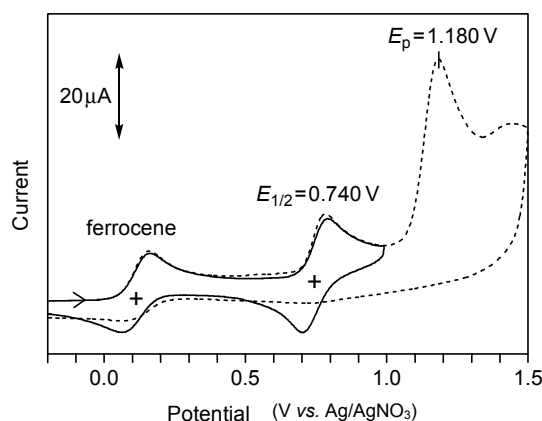
3. Experimental Section

3.1. General

Anhydrous solvents used for synthesis were prepared by standard methods. Other reagents were used as received, unless otherwise noted. Preparative gel permeation chromatography was performed in a recycle mode using Japan Analytical Industry JAIGEL 1H and 2H polystyrene columns, which were connected in a series.

^{1}H-NMR spectra were obtained using either a JEOL AL400 (400 MHz) or a Varian Mercury-300 (300 MHz) instrument. ^{13}C-NMR spectra were measured using a Varian Mercury 300 (75.5 MHz) instrument. High-resolution mass spectra were obtained using a JEOL JMS 700 spectrometer.

The IR spectra of neat samples were obtained with a Thermo-Mattson Infinity spectrometer using a drop-cast film prepared from a CHCl$_3$ solution (5 mM) on a KBr plate at room temperature. The polarization modulation-infrared reflection absorption spectroscopy (PM-IRRAS) spectra were recorded using the same instrument equipped with a HgCdTe detector cooled with liquid N$_2$ and a photoelastic modulator (Hinds, PEM-90) with an optical layout similar to that reported in the literature [56]. The signal was demodulated with a synchronous sampling demodulator (GWC Instruments). The differential reflectance was numerically converted to absorbance. All measurements were performed under an ambient atmosphere at room temperature.

3.2. Synthesis of 1-[4-(2,2'-Bithiophen-5-yl)phenyl]-3,5,7-tris(mercaptomethyl)adamantane (**3a**)

5-(Tributylstannyl)-2,2'-bithiophene (**5a**) [40]: To a solution of 2,2'-bithiophene (0.291 g, 1.75 mmol) in THF (25 mL) was added 1.25 mL of BuLi (1.54 M in hexane) over 5 min at −78 °C, and the mixture

was stirred at this temperature for 30 min. Tributyltin chloride (0.69 g, 2.1 mmol) was added, and the mixture was stirred for 40 min at −78 °C and then for 12 h at room temperature. The mixture was quenched with saturated. NH$_4$Cl, and the product was extracted with ether. The ether solution was dried (MgSO$_4$) and evaporated, and the residue was purified by gel permeation chromatography (CHCl$_3$) to give **5a** as a colorless oil (0.659 g, 83%): ^{1}H-NMR (CDCl$_3$, 300 MHz) δ 0.90 (t, *J* = 7.2 Hz, 9H), 1.09–1.14 (m, 6H), 1.35 (sext, *J* = 7.2 Hz, 6H), 1.56–1.61 (m, 6H), 6.98 (dd, *J* = 5.3, 3.5 Hz, 1H), 7.05 (d, *J* = 3.3 Hz, 1H), 7.14–7.17 (m, 2H), 7.28 (d, *J* = 3.3 Hz, 1H). ^{13}C-NMR (CDCl$_3$, 75.5 MHz) δ 10.9, 13.6, 27.2, 28.9, 123.4, 123.9, 124.9, 127.7, 136.0, 136.5, 137.7, 142.7.

1-[4-(2,2′-Bithiophen-5-yl)phenyl]-3,5,7-tris(acetylthiomethyl)adamantane (**6a**): THF (2.5 mL) was added to a mixture of tris(thioacetate) **4** [26] (45.9 mg, 0.0762 mmol), **5a** (59.1 mg, 0.130 mmol) and Pd(PPh$_3$)$_4$ (26.4 mg, 0.0228 mmol), and the mixture was stirred at 70 °C for 21 h under an argon atmosphere. The mixture was quenched with water, and the product was extracted with ether. The ether solution was washed with 10% NaCl and dried (MgSO$_4$). The solvent was evaporated, and the residue was purified by gel permeation chromatography (CHCl$_3$) to give **6a** as a colorless oil (13.6 mg, 28%): ^{1}H-NMR (CDCl$_3$, 400 MHz) δ 1.24 (d, *J* = 12.6 Hz, 3H), 1.28 (d, *J* = 11.9 Hz, 3H), 1.55 (s, 6H), 2.36 (s, 9H), 2.86 (s, 6H), 7.03 (dd, *J* = 5.1, 3.6 Hz, 1H), 7.13 (d, *J* = 3.9 Hz, 1H), 7.18–7.20 (m, 2H), 7.21 (dd, *J* = 5.1, 1.0 Hz, 1H), 7.30 (d, *J* = 8.5 Hz, 2H), 7.54 (d, *J* = 8.5 Hz, 2H). ^{13}C-NMR (CDCl$_3$, 75.5 MHz) δ 30.7, 35.8, 38.3, 41.0, 43.7, 45.4, 123.48, 123.53, 124.3, 124.5, 125.49, 125.53, 127.8, 131.9, 136.4, 137.4, 142.8, 148.0, 195.3. HRMS (EI+) *m/z* calcd. for C$_{33}$H$_{36}$O$_3$S$_5$ (M$^+$) 640.1268, found 640.1262.

1-[4-(2,2′-Bithiophen-5-yl)phenyl]-3,5,7-tris(mercaptomethyl)adamantane (**3a**): A solution of tris(thioacetate) **6a** (8.2 mg, 0.013 mmol) in THF (3.5 mL) was added to a stirred suspension of LiAlH$_4$ (25.6 mg, 0.675 mmol) in THF (1 mL) over a period of 5 min. The reaction mixture was stirred at 0 °C for 1 h and quenched by the addition of 10% HCl (1.5 mL). The product was extracted with CH$_2$Cl$_2$, and the organic layer was washed with 10% NaCl and dried (MgSO$_4$). The solvent was evaporated to give **3a** as a colorless oil (6.2 mg, 94%): ^{1}H-NMR (CDCl$_3$, 400 MHz) δ 1.21 (t, *J* = 8.8 Hz, 3H), 1.31 (d, *J* = 12.4 Hz, 3H), 1.35 (d, *J* = 12.1 Hz, 3H), 1.61 (s, 6H), 2.49 (d, *J* = 9.0 Hz, 6H), 7.03 (dd, *J* = 5.1, 3.6 Hz, 1H), 7.14 (d, *J* = 3.9 Hz, 1H), 7.19–7.23 (m, 3H), 7.38 (d, *J* = 8.5 Hz, 2H), 7.56 (d, *J* = 8.5 Hz, 2H). ^{13}C-NMR (CDCl$_3$, 75.5 MHz) δ 35.9, 37.5, 38.4, 43.1, 45.4, 123.49, 123.52, 124.3, 124.5, 125.5, 125.6, 127.8, 131.9, 136.4, 137.4, 142.8, 148.4. HRMS (EI+) *m/z* calcd. for C$_{27}$H$_{30}$S$_5$ (M$^+$) 514.0951, found 514.0944.

3.3. Synthesis of 1-[4-(5′-Phenyl-2,2′-bithiophen-5-yl)phenyl]-3,5,7-tris(mercaptomethyl)adamantane (**3b**)

5-Phenyl-2,2′-bithiophene [57]: A DMF solution (2.5 mL) of bromobenzene (105 mg, 0.67 mmol) was added to a mixture of Pd(PPh$_3$)$_4$ (22.4 mg, 0.0194 mmol) and CuO (28.4 mg, 0.357 mmol) under an argon atmosphere. A DMF solution (1 mL) of **5a** (153 mg, 0.336 mmol) was added at 100 °C, and the mixture was stirred at 100 °C for 1 h, filtered through a short SiO$_2$ column and evaporated. The residue was purified by gel permeation chromatography (CHCl$_3$) to give 5-phenyl-2,2′-bithiophene as a yellow solid (71.5 mg, 88%). ^{1}H-NMR (CDCl$_3$, 300 MHz) δ 7.01 (dd, *J* = 5.2, 3.6 Hz, 1H), 7.12 (d, *J* = 3.6 Hz, 1H), 7.16–7.21 (m, 3H), 7.27 (d, *J* = 7.5 Hz, 1H), 7.36 (t, *J* = 7.8 Hz, 2H), 7.58 (d, *J* = 7.8 Hz, 2H).

¹³C-NMR (CDCl₃, 75.5 MHz) δ 123.6, 123.7, 124.3, 124.5, 125.5, 127.5, 127.8, 128.9, 134.0, 136.6, 137.4, 143.0.

5-(Tributylstannyl)-5′-phenyl-2,2′-bithiophene (**5b**): To a solution of 5-phenyl-2,2′-bithiophene (71.5 mg, 0.295 mmol) in THF (5 mL) was added 0.22 mL of BuLi (1.6 M in hexane) over 5 min at −78 °C, and the mixture was stirred at this temperature for 30 min. Tributyltin chloride (0.17 g, 0.52 mmol) was added, and the mixture was stirred for 40 min at −78 °C and for 19 h at room temperature. The mixture was quenched with sat. NH₄Cl, and the product was extracted with ether. The ether solution was dried (MgSO₄) and evaporated, and the residue was purified by gel permeation chromatography (CHCl₃) to give **5b** as a yellow oil (0.147 g, 94%): ¹H-NMR (CDCl₃, 300 MHz) δ 0.91 (t, *J* = 7.4 Hz, 9H), 1.10–1.15 (m, 6H), 1.35 (sext, *J* = 7.3 Hz, 6H), 1.54–1.62 (m, 6H), 7.07 (d, *J* = 3.3 Hz, 1H), 7.13 (d, *J* = 3.6 Hz, 1H), 7.21 (d, *J* = 3.9 Hz, 1H), 7.27 (d, *J* = 7.5 Hz, 1H), 7.31 (d, *J* = 3.3 Hz, 1H), 7.36 (t, *J* = 7.5 Hz, 2H), 7.59 (d, *J* = 7.5 Hz, 2H). ¹³C-NMR (CDCl₃, 75.5 MHz) δ 10.9, 13.7, 27.3, 28.9, 123.7, 124.3, 124.8, 125.5, 127.4, 128.9, 134.2, 136.1, 136.8, 137.0, 142.6, 142.7.

1-[4-(5′-Phenyl-2,2′-bithiophen-5-yl)phenyl]-3,5,7-tris(acetylthiomethyl)adamantane (**6b**): THF (4.5 mL) was added to a mixture of tris(thioacetate) **4** [26] (77.9 mg, 0.129 mmol), **5b** (86.2 mg, 0.162 mmol) and Pd(PPh₃)₄ (30.0 mg, 0.0260 mmol), and the mixture was stirred at 70 °C for 22 h under an argon atmosphere. The mixture was quenched with water, and the product was extracted with ether. The ether solution was washed with 10% NaCl and dried (MgSO₄). The solvent was evaporated, and the residue was purified by gel permeation chromatography (CHCl₃) to give **6b** as a yellow solid (20.6 mg, 22%): ¹H-NMR (CDCl₃, 300 MHz) δ 1.23 (d, *J* = 12.6 Hz, 3H), 1.28 (d, *J* = 12.3 Hz, 3H), 1.55 (s, 6H), 2.36 (s, 9H), 2.86 (s, 6H), 7.15 (d, *J* = 3.6 Hz, 1H), 7.16 (d, *J* = 3.9 Hz, 1H), 7.20 (d, *J* = 3.9 Hz, 1H), 7.24 (d, *J* = 3.6 Hz, 1H), 7.28–7.32 (m, 3H), 7.39 (d, *J* = 7.5 Hz, 2H), 7.54 (d, *J* = 8.4 Hz, 2H), 7.61 (d, *J* = 8.4 Hz, 2H). ¹³C-NMR (CDCl₃, 75.5 MHz) δ 30.7, 35.8, 38.3, 41.0, 43.7, 45.4, 123.6, 123.8, 124.40, 124.45, 125.52, 125.55, 125.57, 127.6, 128.9, 131.9, 134.0, 136.4, 136.7, 142.9, 143.0, 148.1, 195.3. HRMS (EI+) *m/z* calcd. for C₃₉H₄₀O₃S₅ (M⁺) 716.1581, found 716.1547.

1-[4-(5′-Phenyl-2,2′-bithiophen-5-yl)phenyl]-3,5,7-tris(mercaptomethyl)adamantane (**3b**): A solution of tris(thioacetate) **6b** (20.6 mg, 0.0287 mmol) in THF (6 mL) was added to a stirred suspension of LiAlH₄ (86.5 mg, 2.28 mmol) in THF (2.5 mL) over a period of 10 min. The reaction mixture was stirred at 0 °C for 1 h and quenched by the addition of 10% HCl (2 mL). The product was extracted with CH₂Cl₂, and the organic layer was washed with water and dried (MgSO₄). The solvent was evaporated, and the residue was purified by flash column chromatography on silica gel (CH₂Cl₂) to give **3b** as a yellow solid (14.7 mg, 87%): ¹H-NMR (CDCl₃, 300 MHz) δ 1.21 (t, *J* = 8.7 Hz, 3H), 1.32 (s, 6H), 1.61 (s, 6H), 2.49 (d, *J* = 9.0 Hz, 6H), 7.16 (d, *J* = 3.9 Hz, 1H), 7.17 (d, *J* = 3.9 Hz, 1H), 7.21 (d, *J* = 3.6 Hz, 1H), 7.24 (d, *J* = 3.9 Hz, 1H), 7.29–7.41 (m, 5H), 7.56 (d, *J* = 8.7 Hz, 2H), 7.61 (d, *J* = 8.4 Hz, 2H). ¹³C-NMR (CDCl₃, 75.5 MHz) δ 35.9, 37.5, 38.5, 43.1, 45.5, 123.6, 123.8, 124.39, 124.44, 125.51, 125.55, 125.58, 127.6, 128.9, 131.9, 134.0, 136.4, 136.7, 142.8, 143.0, 148.4. HRMS (FAB+) *m/z* calcd. for C₃₃H₃₄S₅ (M⁺) 590.1264, found 590.1273.

3.4. Preparation of the Self-Assembled Monolayer on a Au(111) Substrate

Gold (99.99%) was vapor-deposited on freshly cleaved mica sheets (0.05 mm thickness, 6 cm × 6 cm). The mica was pre-baked at 580 °C under high vacuum (<10^{-3} Pa) for at least 6 h. The deposition was carried out at this temperature with an evaporation rate of 1.0–1.5 nm·s^{-1} until a gold thickness of 200 ± 5 nm was reached. The obtained substrate was cut into 1 cm × 2 cm pieces and annealed at 530 °C in a furnace for 8 h under air to remove the surface contamination and to minimize defects. The hot pieces were quenched in Millipore purified water (resistivity >18 MΩ·cm, Millipore Simplicity 185 Water System). STM analysis of the gold film, thus prepared, showed the formation of large Au(111) terraces. The substrate was consecutively rinsed with EtOH and AcOEt and immersed in a 0.1 mM solution of **3a** in AcOEt. After 24 h, or longer, in the dark, the substrate was rinsed with pure AcOEt and dried under an ambient atmosphere. The SAM of **3b** was prepared in a similar manner using CH_2Cl_2 instead of AcOEt.

3.5. Cyclic Voltammetry

A surface-modified gold substrate was mounted at the bottom of a cone-shaped cell using an O-ring and a clamp to serve as a working electrode. The area of the electrode exposed to the electrolyte was 0.152 cm^2 (4.4 mm diameter circle). Reductive desorption was recorded with aqueous 0.5 M KOH using a Ag/AgCl/sat. KCl reference electrode and a platinum wire counter electrode. Oxidative scans were conducted in a CH_2Cl_2 solution containing 0.1 M tetrabutylammonium perchlorate (TBAP) using a Ag/AgNO$_3$ (0.01 M in CH_3CN) reference electrode and a platinum wire counter electrode. A Luggin capillary (0.5 mm bore) was placed at a distance of about 1 mm from the surface of the working electrode in order to minimize the IR drop in the solution. The electrolyte solution in the cell was deaerated by bubbling argon for 10 min before scanning. Voltammograms were recorded on a BAS 100B electrochemical analyzer.

3.6. Theoretical Calculations

Density functional theory (DFT) calculations [58] were performed using the Gaussian 03 program [59]. Geometry optimization was carried out at the B3LYP/6-31G(d) level. The resultant geometries were verified by frequency calculations to have no imaginary frequencies.

4. Conclusions

Dyads **3a** and **3b**, prepared from bithiophene and adamantane tripodal trithiol, formed SAMs on Au(111) via three-point adsorption, as evidenced by PM-IRRAS measurements and the charge of reductive desorption. A reversible cyclic voltammogram for the single-electron oxidation was obtained by capping the terminal thiophene ring with a phenyl group. An increase in the two-dimensional bulkiness due to the possible *anti-syn* conformational fluctuation resulted in surface coverage that was lower than that observed for a ferrocene-terminated analogue **2**. This is in contrast to the fact that *n*-alkanethiols form closely packed SAMs, in which flexible alkyl chains are fixed at a linear conformation to maximize the intermolecular affinity. The adamantane tripod permits self-assembly in a well-controlled manner and serves as a rigid junction between a device molecule and a metal

electrode. The present results provides insight into the molecular geometry of oligothiophene SAMs, which are promising systems for organic optoelectronic devices.

Supplementary Materials

Supplementary materials can be accessed at http://www.mdpi.com/1420-3049/19/9/15298/s1.

Acknowledgments

Author Contributions

Toshikazu Kitagawa and Koichi Komatsu designed the study and analyzed the data. Hiroaki Matsubara and Toshikazu Kitagawa performed the experiments. Takao Okazaki executed the theoretical calculations. Toshikazu Kitagawa wrote the manuscript.

Conflicts of Interest

The authors declare no conflict of interest.

References and Notes

1. Ulman, A. Formation and Structure of Self-Assembled Monolayers. *Chem. Rev.* **1996**, *96*, 1533–1554.
2. Poirier, G.E. Characterization of Organosulfur Molecular Monolayers on Au(111) using Scanning Tunneling Microscopy. *Chem. Rev.* **1997**, *97*, 1117–1127.
3. Love, J.C.; Estroff, L.A.; Kriebel, J.K.; Nuzzo, R.G.; Whitesides, G.M. Self-Assembled Monolayers of Thiolates on Metals as a Form of Nanotechnology. *Chem. Rev.* **2005**, *105*, 1103–1169.
4. Kind, M.; Wöll, C. Organic surfaces exposed by self-assembled organothiol monolayers: Preparation, characterization, and application. *Prog. Surf. Sci.* **2009**, *84*, 230–278.
5. Chaki, N.K.; Vijayamohanan, K. Self-assembled monolayers as a tunable platform for biosensor applications. *Biosens. Bioelectron.* **2002**, *17*, 1–12.
6. Gooding, J.J.; Mearns, F.; Yang, W.; Liu, J. Self-Assembled Monolayers into the 21st Century: Recent Advances and Applications. *Electroanalysis* **2003**, *15*, 81–96.
7. Bertin, P.A.; Ahrens, M.J.; Bhavsar, K.; Georganopoulou, D.; Wunder, M.; Blackburn, G.F.; Meade, T.J. Ferrocene and Maleimide-Functionalized Disulfide Scaffolds for Self-Assembled Monolayers on Gold. *Org. Lett.* **2010**, *12*, 3372–3375.
8. Jian, H.; Tour, J.M. En Route to Surface-Bound Electric Field-Driven Molecular Motors. *J. Org. Chem.* **2003**, *68*, 5091–5103.
9. Zheng, X.; Mulcahy, M.E.; Horinek, D.; Galeotti, F.; Magnera, T.F.; Michl, J. Dipolar and Nonpolar Altitudinal Molecular Rotors Mounted on an Au(111) Surface. *J. Am. Chem. Soc.* **2004**, *126*, 4540–4542.

10. Van Delden, R.A.; ter Wiel, M.K.J.; Pollard, M.M.; Vicario, J.; Koumura, N.; Feringa, B.L. Unidirectional molecular motor on a gold surface. *Nature* **2005**, *437*, 1337–1340.

11. Kay, E.R.; Leigh, D.A.; Zerbetto, F. Synthetic Molecular Motors and Mechanical Machines. *Angew. Chem. Int. Ed.* **2007**, *46*, 72–191.

12. Tour, J.M. Molecular Electronics. Synthesis and Testing of Components. *Acc. Chem. Res.* **2000**, *33*, 791–804.

13. Donhauser, Z.J.; Mantooth, B.A.; Kelly, K.F.; Bumm, L.A.; Monnell, J.D.; Stapleton, J.J.; Price, D.W., Jr.; Rawlett, A.M.; Allara, D.L.; Tour, J.M.; *et al*. Conductance Switching in Single Molecules through Conformational Changes. *Science* **2001**, *292*, 2303–2307.

14. Park, J.; Pasupathy, A.N.; Goldsmith, J.I.; Chang, C.; Yaish, Y.; Petta, J.R.; Rinkoski, M.; Sethna, J.P.; Abruña, H.D.; McEuen, P.L.; *et al.* Coulomb blockade and the Kondo effect in single-atom transistors. *Nature* **2002**, *417*, 722–725.

15. Lewis, P.A.; Inman, C.E.; Yao, Y.; Tour, J.M.; Hutchison, J.E.; Weiss, P.S. Mediating Stochastic Switching of Single Molecules Using Chemical Functionality. *J. Am. Chem. Soc.* **2004**, *126*, 12214–12215.

16. McCreery, R.L. Molecular Electronic Junctions. *Chem. Mater.* **2004**, *16*, 4477–4496.

17. Zhu, L.; Tang, H.; Harima, Y.; Yamashita, K.; Hirayama, D.; Aso, Y.; Otsubo, T. Electrochemical properties of self-assembled monolayers of tripod-shaped molecules and their applications to organic light-emitting diodes. *Chem. Commun.* **2001**, 1830–1831.

18. Hirayama, D.; Takimiya, K.; Aso, Y.; Otsubo, T.; Hasobe, T.; Yamada, H.; Imahori, H.; Fukuzumi, S.; Sakata, Y. Large Photocurrent Generation of Gold Electrodes Modified with [60]Fullerene-Linked Oligothiophenes Bearing a Tripodal Rigid Anchor. *J. Am. Chem. Soc.* **2002**, *124*, 532–533.

19. Zhu, L.; Tang, H.; Harima, Y.; Yamashita, K.; Aso, Y.; Otsubo, T. Enhanced hole injection in organic light-emitting diodes consisting of self-assembled monolayer of tripod-shaped π-conjugated thiols. *J. Mater. Chem.* **2002**, *12*, 2250–2254.

20. Otsubo, T.; Aso, Y.; Takimiya, K. Functional oligothiophenes as advanced molecular electronic materials. *J. Mater. Chem.* **2002**, *12*, 2565–2575.

21. Ie, Y.; Hirose, T.; Nakamura, H.; Kiguchi, M.; Takagi, N.; Kawai, M.; Aso, Y. Nature of Electron Transport by Pyridine-Based Tripodal Anchors: Potential for Robust and Conductive Single-Molecule Junctions with Gold Electrodes. *J. Am. Chem. Soc.* **2011**, *133*, 3014–3022.

22. Hirose, T.; Ie, Y.; Aso, Y. Synthesis of Tripodal-anchor Units Having Pyridine or Amine Functional Groups and Their Adsorption Behavior on Metal Electrodes. *Chem. Lett.* **2011**, *40*, 204–205.

23. Kitagawa, T.; Idomoto, Y.; Matsubara, H.; Hobara, D.; Kakiuchi, T.; Okazaki, T.; Komatsu, K. Rigid Molecular Tripod with an Adamantane Framework and Thiol Legs. Synthesis and Observation of an Ordered Monolayer on Au(111). *J. Org. Chem.* **2006**, *71*, 1362–1369.

24. Katano, S.; Kim, Y.; Matsubara, H.; Kitagawa, T.; Kawai, M. Hierarchical Chiral Framework Based on a Rigid Adamantane Tripod on Au(111). *J. Am. Chem. Soc.* **2007**, *129*, 2511–2515.

25. Katano, S.; Kim, Y.; Kitagawa, T.; Kawai, M. Self-Assembly and Scanning Tunneling Microscopy Tip-Induced Motion of Ferrocene Adamantane Trithiolate Adsorbed on Au(111). *Jpn. J. Appl. Phys.* **2008**, *47*, 6156–6159.

26. Kitagawa, T.; Matsubara, H.; Komatsu, K.; Hirai, K.; Okazaki, T.; Hase, T. Ideal Redox Behavior of the High-Density Self-Assembled Monolayer of a Molecular Tripod on a Au(111) Surface with a Terminal Ferrocene Group. *Langmuir* **2013**, *29*, 4275–4282.

27. Katano, S.; Kim, Y.; Kitagawa, T.; Kawai, M. Tailoring electronic states of a single molecule using adamantane-based molecular tripods. *Phys. Chem. Chem. Phys.* **2013**, *15*, 14229–14233.

28. Fox, M.A.; Whitesell, J.K.; McKerrow, A.J. Fluorescence and Redox Activity of Probes Anchored through an Aminotrithiol to Polycrystalline Gold. *Langmuir* **1998**, *14*, 816–820.

29. Kittredge, K.W.; Minton, M.A.; Fox, M.A.; Whitesell, J.K. α-Helical Polypeptide Films Grown From Sulfide or Thiol Linkers on Gold Surfaces. *Helv. Chim. Acta* **2002**, *85*, 788–798.

30. Wei, L.; Padmaja, K.; Youngblood, W.J.; Lysenko, A.B.; Lindsey, J.S.; Bocian, D.F. Diverse Redox-Active Molecules Bearing Identical Thiol-Terminated Tripodal Tethers for Studies of Molecular Information Storage. *J. Org. Chem.* **2004**, *69*, 1461–1469.

31. Wei, L.; Tiznado, H.; Liu, G.; Padmaja, K.; Lindsey, J.S.; Zaera, F.; Bocian, D.F. Adsorption Characteristics of Tripodal Thiol-Functionalized Porphyrins on Gold. *J. Phys. Chem. B* **2005**, *109*, 23963–23971.

32. Weidner, T.; Zharnikov, M.; Hoßbach, J.; Castner, D.G.; Siemeling, U. Adamantane-Based Tripodal Thioether Ligands Functionalized with a Redox-Active Ferrocenyl Moiety for Self-Assembled Monolayers. *J. Phys. Chem. C* **2010**, *114*, 14975–14982.

33. Singhana, B.; Rittikulsittichai, S.; Lee, T.R. Tridentate Adsorbates with Cyclohexyl Headgroups Assembled on Gold. *Langmuir* **2013**, *29*, 561–569.

34. Singhana, B.; Jamison, A.C.; Hoang, J.; Lee, T.R. Self-Assembled Monolayer Films Derived from Tridentate Cyclohexyl Adsorbates with Alkyl Tailgroups of Increasing Chain Length. *Langmuir* **2013**, *29*, 14108–14116.

35. Ng, M.K.; Lee, D.C.; Yu, L. Molecular Diodes Based on Conjugated Diblock Co-oligomers. *J. Am. Chem. Soc.* **2002**, *124*, 11862–11863.

36. Martin, P.; Rocca, M.L.D.; Anthore, A.; Lafarge, P.; Lacroix, J.C. Organic Electrodes Based on Grafted Oligothiophene Units in Ultrathin, Large-Area Molecular Junctions. *J. Am. Chem. Soc.* **2012**, *134*, 154–157.

37. Wan, D.; Yuan, S.; Neoh, K.G.; Kang, E.T. Surface Functionalization of Copper via Oxidative Graft Polymerization of 2,2′-Bithiophene and Immobilization of Silver Nanoparticles for Combating Biocorrosion. *ACS Appl. Mater. Interfaces* **2010**, *2*, 1653–1662.

38. Malenfant, P.R.L.; Jayaraman, M.; Fréchet, J.M.J. Dendrimer-Supported Oligothiophene Synthesis: Aliphatic Ether Dendrimers in the Preparation of Oligothiophenes with Minimal Substitution. *Chem. Mater.* **1999**, *11*, 3420–3422.

39. Morin, J.F.; Leclerc, M. Syntheses of Conjugated Polymers Derived from *N*-Alkyl-2,7-carbazoles. *Macromolecules* **2001**, *34*, 4680–4682.

40. Idzik, K.R.; Frydel, J.; Beckert, R.; Ledwon, P.; Lapkowski, M.; Fasting, C.; Müller, C.; Licha, T. Synthesis and electrochemical properties of tetrathienyl-linked branched polymers with various aromatic cores. *Electrochim. Acta* **2012**, *79*, 154–161.

41. Walczak, M.M.; Popenoe, D.D.; Deinhammer, R.S.; Lamp, B.D.; Chung, C.; Porter, M.D. Reductive Desorption of Alkanethiolate Monolayers at Gold: A Measure of Surface Coverage. *Langmuir* **1991**, *7*, 2687–2693.

42. Widrig, C.A.; Chung, C.; Porter, M.D. The electrochemical desorption of n-alkanethiol monolayers from polycrystalline Au and Ag electrodes. *J. Electroanal. Chem*. **1991**, *310*, 335–359.

43. Yang, D.F.; Wilde, C.P.; Morin, M. Studies of the Electrochemical Removal and Efficient Re-formation of a Monolayer of Hexadecanethiol Self-Assembled at an Au(111) Single Crystal in Aqueous Solutions. *Langmuir* **1997**, *13*, 243–249.

44. Imabayashi, S.; Iida, M.; Hobara, D.; Feng, Z.Q.; Niki, K.; Kakiuchi, T. Reductive desorption of carboxylic-acid-terminated alkanethiol monolayers from Au(111) surfaces. *J. Electroanal. Chem.* **1997**, *428*, 33–38.

45. Hobara, D.; Miyake, K.; Imabayashi, S.; Niki, K.; Kakiuchi, T. In-Situ Scanning Tunneling Microscopy Imaging of the Reductive Desorption Process of Alkanethiols on Au(111). *Langmuir* **1998**, *14*, 3590–3596.

46. Kakiuchi, T.; Usui, H.; Hobara, D.; Yamamoto, M. Voltammetric Properties of the Reductive Desorption of Alkanethiol Self-Assembled Monolayers from a Metal Surface. *Langmuir* **2002**, *18*, 5231–5238.

47. Eggers, P.K.; Zareie, H.M.; Paddon-Row, M.N.; Gooding, J.J. Structure and Properties of Redox Active Self-Assembled Monolayers Formed from Norbornylogous Bridges. *Langmuir* **2009**, *25*, 11090–11096.

48. A slightly higher energy (2.8 kJ·mol^{-1}) of the *syn* conformer was also reported for parent 2,2′-bithiophene: Diaz-Quijada, G.A.; Weinberg, N.; Holdcroft, S.; Pinto, B.M. Investigation of Barriers To Conformational Interchange in Oligothiophenes and Oligo(Thienyl)furans. *J. Phys. Chem. A* **2002**, *106*, 1266–1276.

49. Wakamiya, A.; Nishinaga, T.; Komatsu, K. The stable radical cation of thiophene annelated with bicyclo[2.2.2]octene and its reaction with triplet oxygen to give a protonated cation of 2-butene-1,4-dione derivative. *Chem. Commun.* **2002**, 1192–1193.

50. Bard, A.J.; Faulkner, L.R. *Electrochemical Methods: Fundamentals and Applications*, 2nd ed.; John Wiley and Sons: New York, NY, USA, 2001; pp. 590–593.

51. Dudek, S.P.; Sikes, H.D.; Chidsey, C.E.D. Synthesis of Ferrocenethiols Containing Oligo(phenylenevinylene) Bridges and Their Characterization on Gold Electrodes. *J. Am. Chem. Soc.* **2001**, *123*, 8033–8038.

52. Lee, L.Y.S.; Sutherland, T.C.; Rucareanu, S.; Lennox, R.B. Ferrocenylalkylthiolates as a Probe of Heterogeneity in Binary Self-Assembled Monolayers on Gold. *Langmuir* **2006**, *22*, 4438–4444.

53. Guo, Y.; Zhao, J.; Zhu, J. Study on the intermolecular interactions between the functional moieties in ferrocene-terminated alkanethiol self-assembled monolayer on gold. *Thin Solid Films* **2008**, *516*, 3051–3057.

54. The large current decrease in the second cycle may be ascribed to a double layer reorganization.

55. Van Haare, J.A.E.H.; van Boxtel, M.; Janssen, R.A.J. π-Dimers of Prototype High-Spin Polaronic Oligomers. *Chem. Mater.* **1998**, *10*, 1166–1175.

56. Barner, B.J.; Green, M.J.; Saez, E.I.; Corn, R.M. Polarization modulation Fourier transform infrared reflectance measurements of thin films and monolayers at metal surfaces utilizing real-time sampling electronics. *Anal. Chem.* **1991**, *63*, 55–60.

57. Yokooji, A.; Satoh, T.; Miura, M.; Nomura, M. Synthesis of 5,5′-diarylated 2,2′-bithiophenes via palladium-catalyzed arylation reactions. *Tetrahedron* **2004**, *60*, 6757–6763.

58. Koch, W.; Holthausen, M.C. *A Chemist's Guide to Density Functional Theory*, 2nd ed.; Wiley-VCH: Weinheim, Germany, 2000.

59. Frisch, M.J.; Trucks, G.W.; Schlegel, H.B.; Scuseria, G.E.; Robb, M.A.; Cheeseman, J.R.; Montgomery, J.A., Jr.; Vreven, T.; Kudin, K.N.; Burant, J.C.; *et al. Gaussian 03*, Revision E.01; Gaussian, Inc.: Wallingford, CT, USA, 2004.

Sample Availability: Not available.